Title: Total synthesis of twenty-five picrotoxanes by virtual library selection

Authors: Chunyu Li,[1,2] Ryan A. Shenvi[1,2,*]

Affiliations: [1]Department of Chemistry, Scripps Research, La Jolla, California 92037, United States; [2]Graduate School of Chemical and Biological Sciences, Scripps Research, La Jolla, California 92037, United States; *Email: rshenvi@scripps.edu

Referenced Single Paragraph Intro. Strong-bond activation refers to the conversion of typically inert functional groups (FG) into reactive ones: e.g. C–H or C–C into C–X.[1] Its application in retrosynthetic analysis[2,3] requires evaluation of strategy (*is it simplifying?*) and feasibility (*will it work?*). However, the feasibility of strong bond cleavage can be difficult to predict due to competing low barrier pathways (e.g. 5–8 kcal/mol)[4,5] in complex molecular environments.[6,7,8] If strong bond activation can be strategically evaluated, accurately calculated and experimentally validated, it can simplify the synthesis of complex molecules.[2,3] Here we build a virtual library of strategic late-stage intermediates en route to diverse picrotoxanes, calculate C–H vs. C–C oxidation preference and experimentally interrogate the predictions. Costly transition state calculations are then simplified to faster parameterizations to explain remote effects on strong bond activation and to devise concise routes to the picrotoxanes[9].

Introduction. The picrotoxanes (**Fig 1a**) occur across diverse plant genera and include at least 102 members, many of which selectively antagonize the *gamma*-aminobutyric acid A receptor ($GABA_AR$),[10] a major neurotransmitter-gated ion channel expressed in the mammalian nervous system.[11] Close homology between $GABA_AR$ and invertebrate receptors[12] has led to the deployment of picrotoxanes against parasitic infection[13] like filariasis.[10] Broader adaptation for medical use,[14] however, has been hampered by their complexity, toxicity[15] and instability.[16] Syntheses of tutin[17,18] corianin[19,20] and coriamyrtin[21,22,23] have required 43 steps (0.0013%), 30 steps (0.27%) and at least 15 steps (0.01%) respectively, and have delivered no analogs. Recently, we identified structural modifications to the flagship member, PXN, that stabilized it against C15 solvolysis and altered its selectivity among ion channels—reducing affinity for mammalian receptors while maintaining potency at invertebrate resistance-to-dieldrin (RDL) receptors.[24] However, we also found that the major kinetic site of hydrolysis was C11, not C15 (**Fig 1a**)[25] as long thought.[26] As a result, congeners that lack a C11 carbonyl, like tutin (**T**, **1**) and corianin (**C**, **2**), should exhibit a longer lifetime in buffer and serum; indeed, tutin persists in blood ($t_{1/2}$ = 10 h) via slow release from its C2-glycosides.[27]

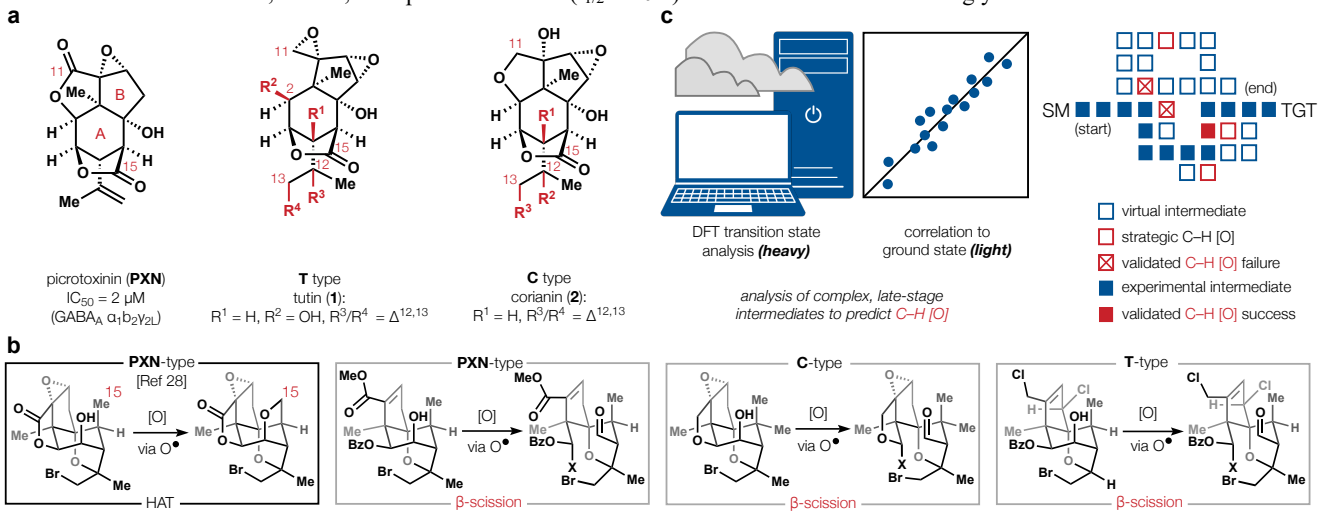

Figure 1. Design, observations and problems. **a**. Picrotoxinin and congeners. **b**. Tactical failure: minor B-ring changes divert 1,5-HAT to a β-scission pathway and prevent access to **T** and **C** classes. **c**. High level DFT and parametrization can sort possible intermediates as a framework to probe pathway prediction in CASP.

Our prior route to PXN relied on C15 methyl oxidation to establish the A-ring lactone bridge. This C–H to O• 1,5 HAT (see **Fig 1b**) required a C–H–O transition state that approached co-linearity (180°) and C–H, O• groups in close proximity (C--O < 2.8 Å)[4,5] Diverse picrotoxane scaffolds met these criteria and therefore seemed ideal subtargets to reach the **T** and **C** classes via 1,5-HAT. Unfortunately, adaptation of our PXN synthesis[28] failed. Only minor changes to the B-ring caused the 1,5-HAT step to instead favor β-scission (**Fig 1b**).[29] This failure of the C–H oxidation step at the tactical level was not predicted by heuristics,[30] basic patterns of reactivity[31,30,32] or existing data.[33,34] These are key features of computer assisted synthesis planning (CASP): an approach to dramatically simplify problems like **1** and **2** with computational algorithms.[35,36,37] To address its shortcomings and avoid a laborious guess-and-check empirical approach, we imagined a DFT module that would evaluate feasible reactivity of an *in silico* library, which could be parameterized to deliver faster predictions (**Fig. 1c**). Among the subset of intermediates predicted to be feasible, standard heuristics could then determine which were strategic.

Results and Discussion. A streamlined entry to the picrotoxanes began with α-vinylation of **4** (0.25 mol% Pd(t-Bu_3P)$_2$, 20:1 dr, >200 mmol, 88%),[38] whereby the axial α-vinyl of **5** allowed stereoselective aldol reaction and dehydration of 2-oxo-methylbutanoate to arrive at **6**. Intramolecular aldol cyclization combined with bromoetherification and Johnson-Lemieux oxidation produced aldehyde **7** in 68% yield (a range of step counts (1-3) avoids unfair contrast to prior work that used different counting conventions). Modified Dong transfer hydroformylation[39] using Ph_2PO_2H as a novel Rh ligand [see SI] proved crucial to synthetic design because the resulting $\Delta^{5,15}$ 1,1-disubstituted alkene allowed unrestricted access to the hindered $\Delta^{3,4}$ alkene without itself undergoing reaction (see **8**). Consequently, osmium-catalyzed dihydroxylation (<5 mol% OsO_4) occurred over 5 h, whereas prior picrotoxane substrates have required stoichiometric osmium (1-10 equiv.) and protracted reaction times (3-7 d, 23-70 °C).[28,40,41] Triene **8** could be isolated or dihydroxylated *in situ* to yield **9a**; alternatively, thexylborane-mediated hydroboration yielded **9b**.

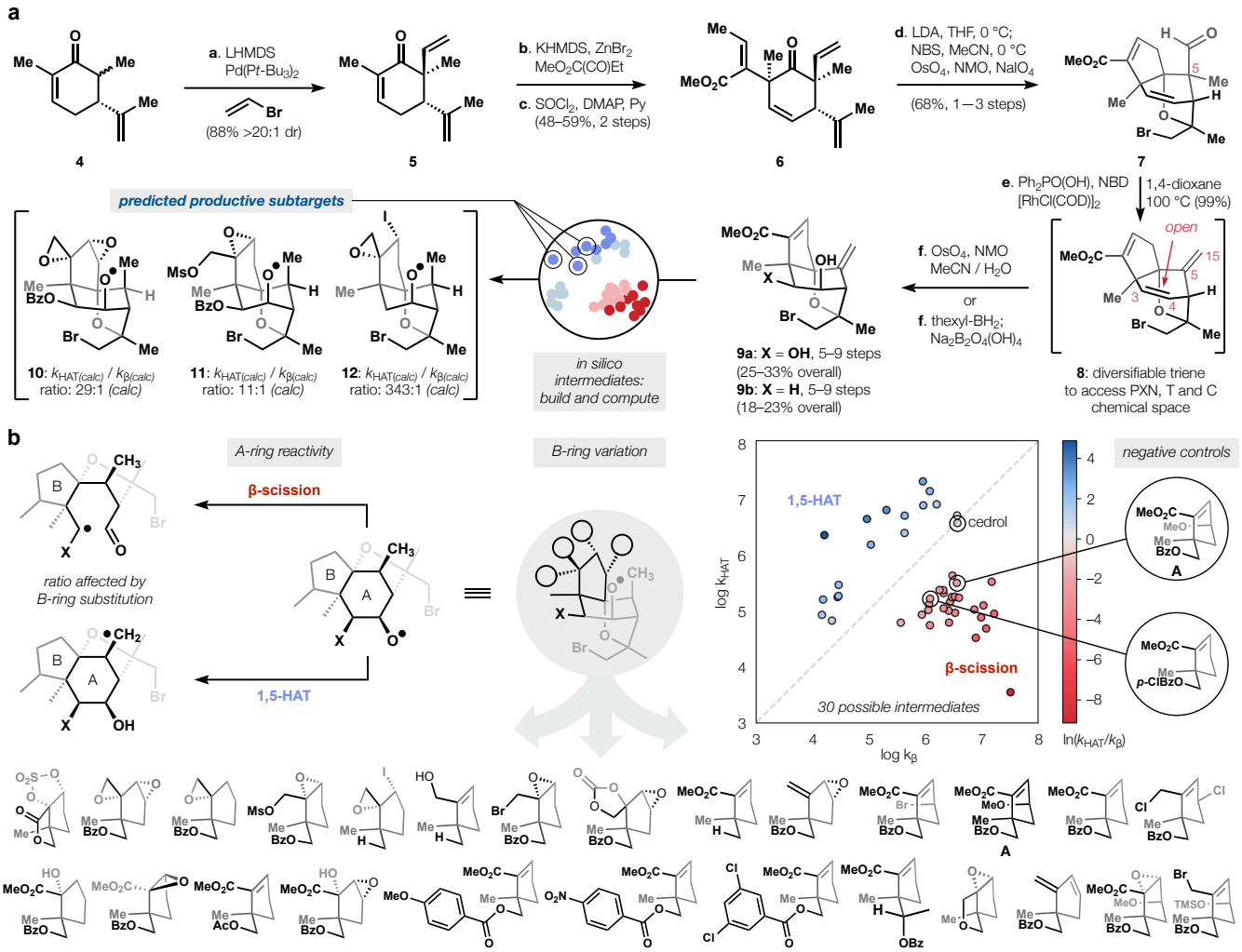

Figure 2. Synthesis entry and virtual library. **a**. Access to divergent intermediates **9a**/**b**. **b.** Calculation of A-ring relative rates based on B-ring substitution identifies possible intermediates.

The two reaction pathways implicated by experiment, 1,5-HAT and β-scission, were modeled with the Gaussian 16 software package using the Scripps Garibaldi cluster (46 TFlops, theoretical peak performance; 17 Terabytes total memory, see SI). Both elementary steps could be accelerated by tunneling along the reaction coordinate[42,43] so that traditional comparisons of Gibbs activation energies were replaced with rate constants using transition-state theory (TST)[44,45] with one dimensional Eckart tunneling correction.[42] The relative preference for 1,5-HAT vs. β-scission is therefore expressed in **Fig 2b** in rates: log k_{HAT},log k_{β} (*avg*. value given if multiple conformers possible). Results from several levels of functional theory were calibrated against experimental data (**Fig 1b**), in addition to literature data for the Suárez reactions of cedrol (*ca.* 2.3-2.7:1 1,5-HAT:β-scission).[46] After calibration, virtual compounds (31 compounds and 51 total conformers) were evaluated at the uM062X-D3 functional level with the 6-311+G(d, p) basis set[47] and SMD solvent model[48].

More than half of the virtual library appeared to favor β-scission, but several members preferred HAT. Among these, the highest-risk/ highest reward subtarget was *bis*-epoxide **10** (**Fig 2a**, calculated ratio of 29:1 HAT:β-scission), which contained the native strained B-ring of tutin itself. Assessment of this calculation would involve a speculative multistep synthesis. If successful, however, it would deliver the (+)-tutin scaffold almost fully formed. This enticing possibility led us to prioritize **10** for synthesis and evaluate the accuracy of theory. Similarly, the unusual epoxy mesylate **11** was calculated to favor HAT over β-scission by 9:1 (*avg.* of conformers) and might easily lead to (+)-corianin **3**. Interestingly, the corresponding bromide was calculated to generate a mixture of HAT and β-scission products from its ensemble of conformers; both the bromide and the mesylate were investigated experimentally. Finally, iodo-epoxide **12**, a motif formed unexpectedly in a prior investigation, indicated strong preference of HAT over β-scission and might lead to C2 deoxy congeners like (+)-coriamyrtin (**13**, see below).

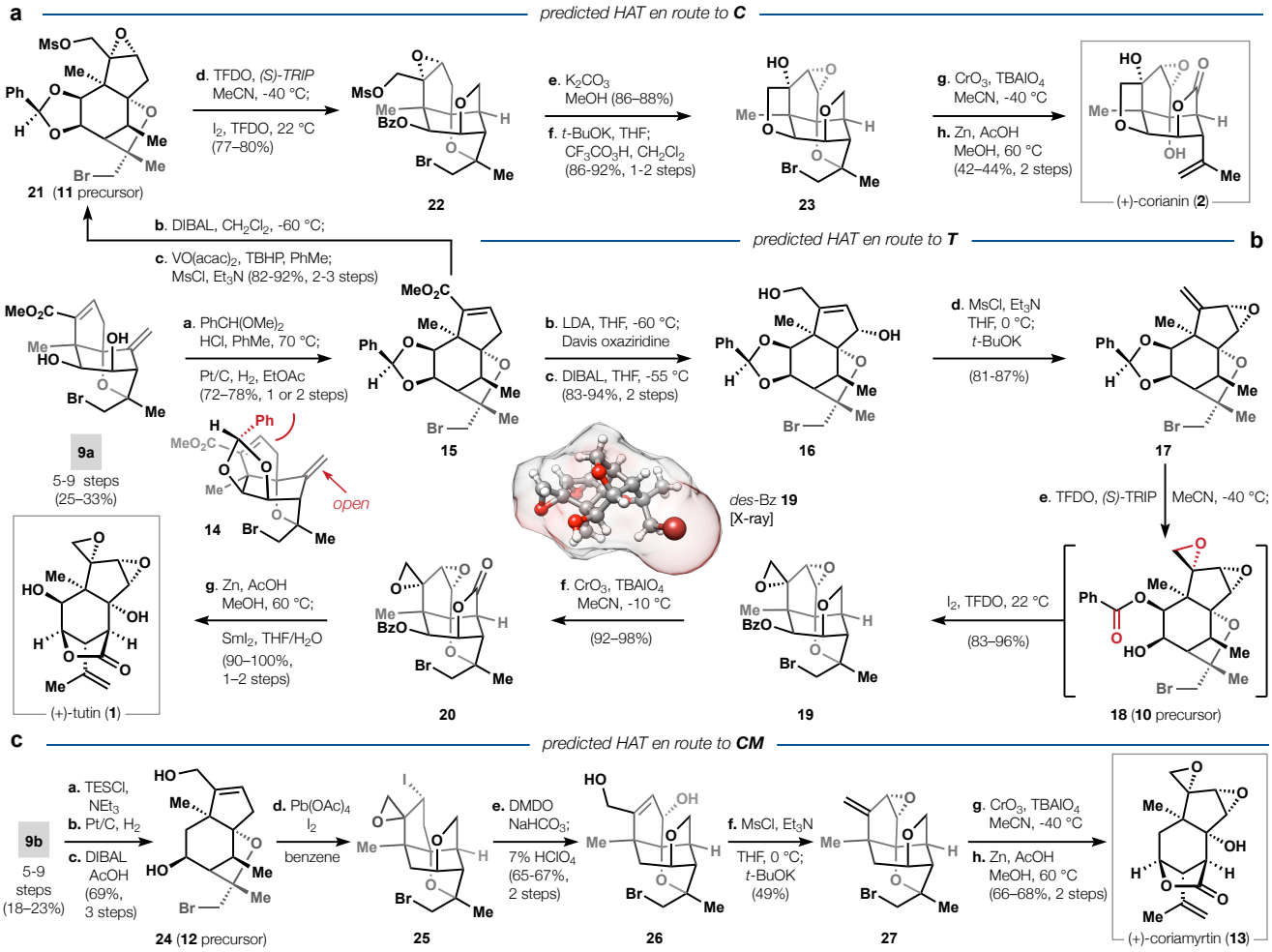

Figure 3. Synthesis of three picrotoxanes using calculated intermediates: **a.** (+)-corianin (**3**), **b**. (+)-tutin (**2**), **c**. (+)-coriamyrtin (**13**). Only a single stereoisomer was isolated in each reaction.

To access HAT substrates from **9a**, we first transketalized to a benzylidene acetal, which formed stereoselectively to position the phenyl ring *endo* to the picrotoxane scaffold (see **14**, **Fig 3**), based on the preferred conformation of the intermediate oxocarbenium. The benzylidene acetal served four roles: 1) to occlude one face of the C5 alkene, 2) to protect the C2 alcohol against competitive Suárez reaction, 3) to promote HAT vs. β-scission as its benzoate ester, as suggested by the calculations in **Fig 2b**, and 4) to slow 1,2-acyl shift (the acetate tended to migrate). First, hydrogenation catalyzed by Pt/C could be carried out *in situ* to yield **15** as a single diastereomer, whereas hydrogenation of **9a** resulted in 1.7:1 dr. Ester deprotonation with LDA and γ-selective oxidation at -60 °C, followed by reduction with DIBAL yielded **16** as a single diastereomer. Sulfene-mediated mesylation,[49] followed by intramolecular allylic substitution[50] arrived at mono-epoxide **16**. Conversion of **16** to **17** occurred by benzylidene acetal C–H oxidation with TFDO to its orthoacetal, which opened selectively to the C2 benzoate in the presence of 5 mol% *(S)*-TRIP[51], whereas achiral acids resulted in regioisomeric mixtures or a strong preference for the C3 benzoate. Extended reaction times caused TFDO to further oxidize $\Delta^{9,10}$ alkene to epoxide **18**, now poised to undergo the Suárez 1,5 HAT predicted for **10** in Figure 2. This reaction could be conducted *in situ* by addition of I_2 to the remaining excess TFDO, likely forming I_2O[52]). The 1,5-HAT etherification product **19** predominated in 83-96% yield (confirmed by X-ray, see *des*-Bz **19**) with no discernible presence of β-scission products by ^{1}H NMR, corresponding well to the calculations. *As a negative control, we subjected β-scission-biased substrate **A** (**Fig 2b**) to the same conditions and found that it generated only aldehydes and no HAT products.* A simple sequence of ether oxidation to bridging lactone **20**[53], followed by β-bromoether reductive cleavage by Zn^0 and benzoate deprotection with SmI_2 and water completed the synthesis of (+)-tutin (**1**) in 12–17 steps and 9.0–18.9% overall. The final benzoate removal proved challenging due to O2-C15 translactonization under basic conditions, and alkene etherification under acidic. Hydride donors yielded only traces of (+)-**1**, but SmI_2, a single electron donor, worked well.

A modification of this sequence accessed (+)-corianin (**2**) via mesylate **21**, itself accessible from **15** by ester reduction, epoxidation and mesylation. The identical sequence developed for **17** in the T-series was applied to mesylate **21**, resulting in acetal oxidation/migration and 1,5-HAT to yield **22** in 80% yield. The apparent HAT:β-scission ratio of 11:1 matched the calculated ratio of 9:1 *(avg)*. Debenzoylation with NaOMe and epoxide isomerization with *t*-BuOK led to an alkene that could be oxidized by CF_3CO_3H to yield **23**, which incorporated the full corianin pattern of cyclopentane oxidation. Completion of (+)-**2** only required monoperoxo chromate oxidation[53] to the bridging lactone and bromoether reductive cleavage, resulting in a 13–20 steps synthesis (3.5–6.7% yield overall).

Finally, we sought to test iodo-epoxide **12** (**Fig 2b**)[54] The allylic alcohol **24** was derived from **9b** via TES silylation to increase steric repulsion on its upper face, followed by alkene hydrogenation, ester reduction and desilylation upon acetic acid quench. Suárez conditions first reacted the allylic alcohol motif to yield an inconsequential 1:1 mixture of diastereomers, which underwent 1,5-HAT instead of β-scission in a >20:1 ratio. Iodide **25** eliminated upon treatment with DMDO to yield an unstable epoxy-alkene, which was hydrated with aqueous perchloric acid to yield **26**. A similar sequence to (+)-tutin (**1**) then completed (+)-coriamyrtin (**13**) in 13–17 overall steps and 2.6–3.5% overall yield.

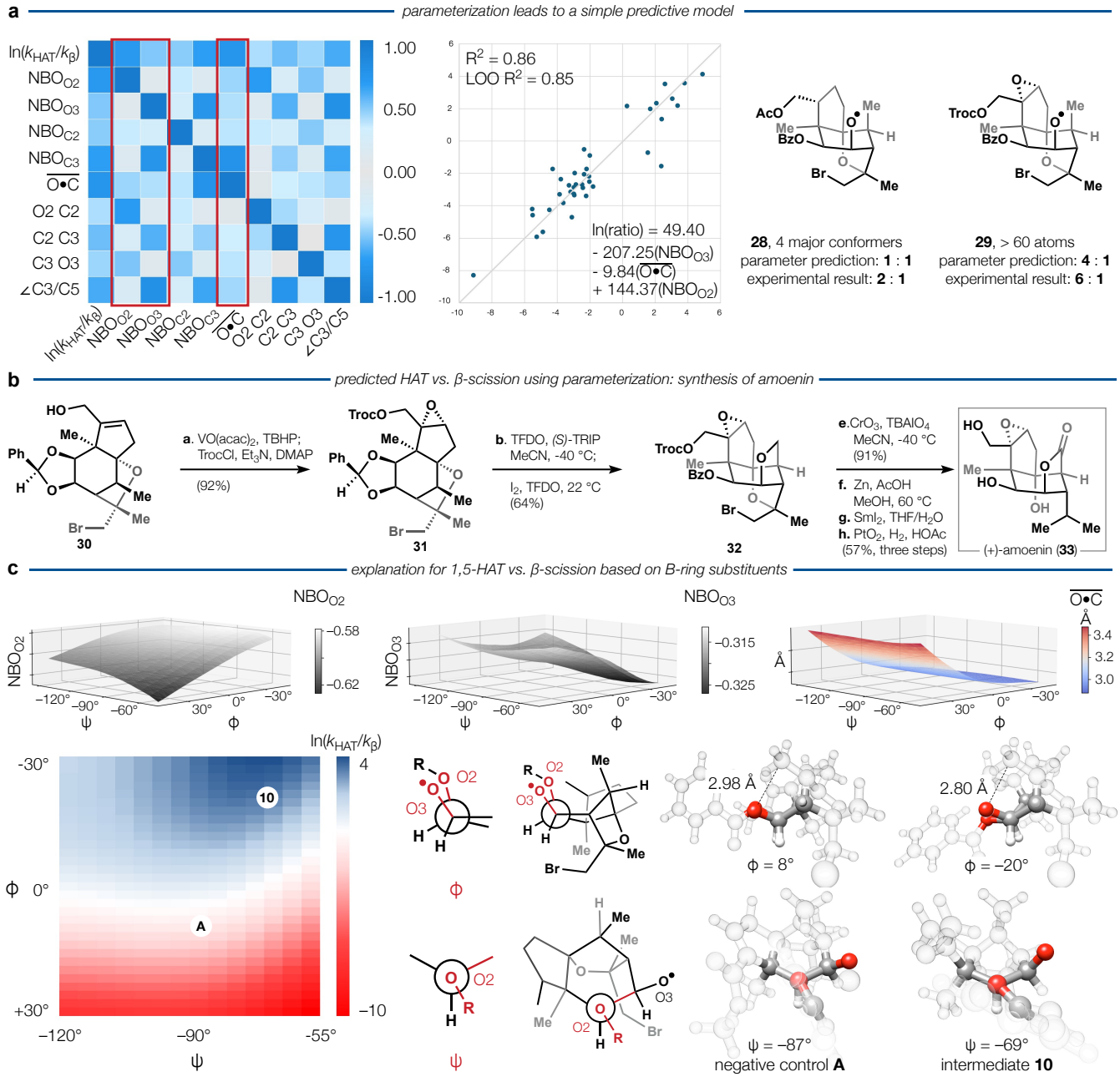

Figure 4. Parametrization and prediction. **a.** Correlation heatmap of 9 parameters leads to a predictive model. **b**. short synthesis of amoenin predicted by parameterization. **c**. ln(k_{HAT}/k_{β}) heatmap defined by φ and ψ.

The successful prediction of selectivity by library members required a high computational cost: multiple days of cluster time for compounds >60 atoms using 3-ζ basis sets.[55] Therefore, we searched for parameters that might accurately predict relative rates of HAT vs. β-scission without transition state or product calculations. A correlation heatmap of selectivity (**Fig 4a**, nine parameters of interatomic distance[5] and atomic charge[56]) and exhaustive regression led O•C interatomic distance ($\overline{O \bullet C}$) and natural bond orbital (NBO) charge at O2 (NBO_{O2}) and O3 (NBO_{O3}) to be selected as non-redundant parameters that correlated to HAT selectivity in a multivariate regression model (0.85 R^2). Increased negative charge on O2 correlated to β-scission rate, whereas increased negative charge on O3 correlated to 1,5-HAT; these could be weighted predictively. This simpler parameterized model required half an hour per compound and predicted that *O*-Troc and O-Ac epoxides **28** and **29** would prefer 1,5-HAT over β-scission at 4:1 and 1:1 ratios, respectively. Experimental ratios—6:1 and 2:1—roughly matched these values (**Fig 4b**) and led to the total synthesis of (+)-amoenin (**31**).

These correlations between structure and rate raised the question of how the B-ring affected NBO_{O2}, NBO_{O3}, and ($\overline{O \bullet C}$). Conformational analysis of the *in silico* library suggested a transmissive effect from the B-ring, whose conformation and substituents controlled two A-ring dihedral angles, ψ and φ (**Fig 4c**). Decreasing values of φ rotated O3 towards C15, enhancing the rate of 1,5-HAT through proximity; ψ and φ together affected NBO_{O3}, where greater charge correlated to faster HAT, likely through polarization effects.[56] Similarly, ψ and φ values directly correlated to O2 negative charge, which increased β-scission, likely due to C• stabilization in the transition state. These relationships created a "sweet spot" of 1,5-HAT selectivity centered at ψ = -70° and φ = -30°; the diepoxy motif of **10**, for example, enforced ψ and φ angles through a B-ring conformation that drove its substituents against the C2 benzoate. In contrast, the B-ring substitution of negative control **A** allowed dihedral angles that led to β-scission. These B-ring features would be challenging to design *a priori* or predict in the absence of calculation.

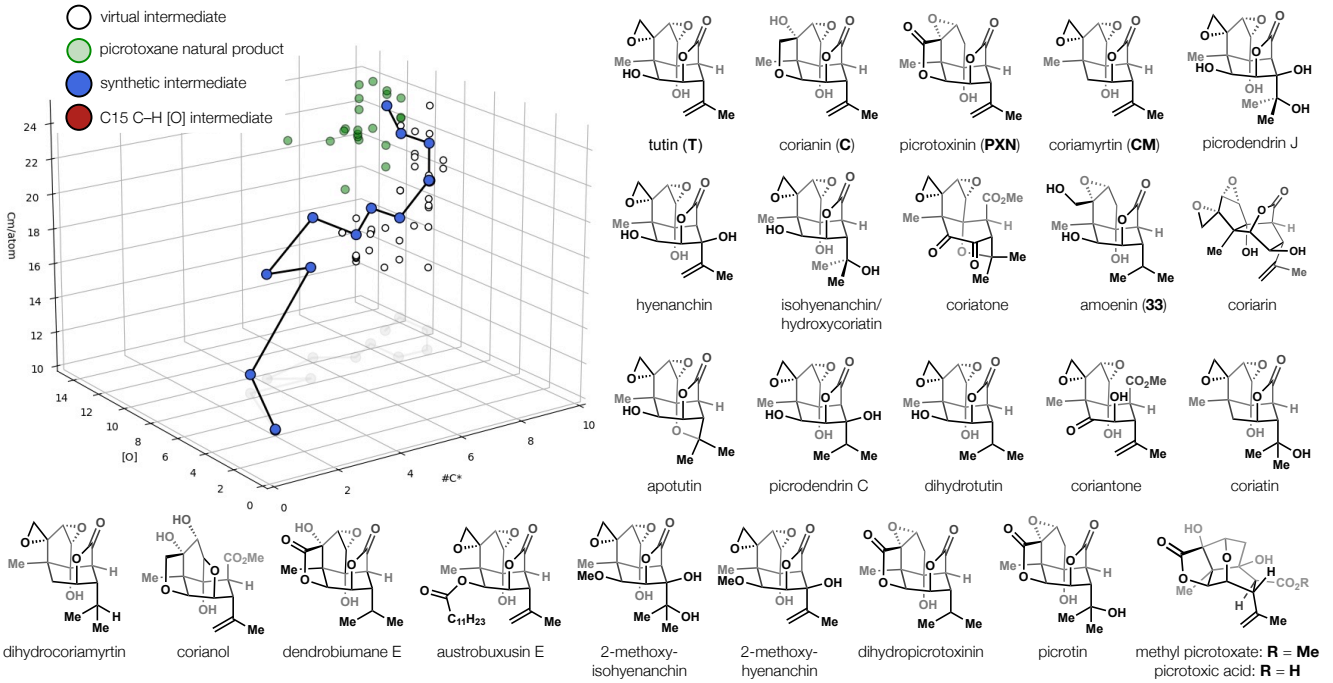

Figure 5. Navigation of chemical space aided by "virtual probes" to guide route selection leads to 25 picrotoxanes.

Conclusion. Computer aided synthesis planning (CASP) holds great promise to speed the production of complex molecules. However, functionally dense targets cannot be predictably analyzed yet,[57] as illustrated here, due to changes in reactivity associated with multiple interacting components. If an algorithm were to map a tutin synthesis onto the pre-existing picrotoxinin synthesis,[28] it would fail (**Fig 1c**). Approaches based on template-matching,[35] language models[37], or database mining[33,34] do not distinguish the features in Figure 2b that lead to success or failure in a multistep route. The solution described here involves a DFT module for steps of low predictability [i.e. thin literature precedent] or few experimental options. The DFT module can be used to generate predictive parameters in a library of restricted size, leading to a multivariate regression model and a larger search space of possible intermediates,[58] providing more opportunities to identify an efficient strategy. This trade-off between specificity and coverage[35] makes sense for complex molecules where the slow step is synthesis, not design. And it makes sense where the exponential "one-to-many" problem[59] of an EXTGT tree[30] is constrained by a transform-based strategy[30] that identifies key subtargets. As late as 1996, the accurate prediction of reaction outcome was deemed "not yet very successful" in the context of synthesis design,[60] but subsequent advances in computational power and software have reduced this to an attainable goal[61] and led to the virtual library search described here. The brevity of this approach has enabled the synthesis of 25 picrotoxanes (**Fig 5** and SI) via efficient navigation of chemical space, where complexity increases in a roughly linear way (tutin synthesis shown) and oxidation can be embedded early, allowing for explosive divergency. We aim to explore these chemotypes as selective ion channel inhibitors, as recently demonstrated with a small library of non-natural picrotoxinin analogs.[24] Many congeners described here lack the labile C11 lactone[25] and may prove to be useful leads to perturb GABAergic signaling.[12–15] These concise syntheses make possible the thorough exploration of picrotoxane chemical space.

Data availability

All data are made available in the main text or the Supporting Information, including experimental procedures, copies of NMR spectra and X-ray structure reports. Structural parameters are available from the Cambridge Crystallographic Data Centre (CCDC) under the following reference numbers: *des*-Bz **19**, 2250952; (+)-tutin (**1**), 2304983; **21**, 2303677.

Code availability

Code used in Fig 2,4 and 5 is in the Supplementary Information.

Acknowledgements. We gratefully acknowledge J. S. Chen and the Scripps Automated Synthesis facility (ASF) for analysis. L. Pasternack, G. J. Kroon and D.-H. Huang are acknowledged for assistance with NMR spectroscopy. M. Gembicky, J. Bailey and the entire UCSD Crystallography Facility are acknowledged for X-ray crystallographic analysis. J.-C. Ducom and L. Dong are acknowledged for assistance with the computing cluster. We thank Dr. Stephen Ting for helpful conversations about statistical modeling. We thank Professors Keary Engle, Tim Cernak and Mr. Di Wang for helpful computational suggestions. Funding was provided by the National Institutes of Health (GM122606) and the Kellogg Scripps Graduate Program (Dale Boger Endowed Graduate Fellowship to C. L.).

References

1. Crabtree, R. H. The organometallic chemistry of alkanes. *Chem. Rev.* **85**, 245–269 (1985).

2. Gutekunst, W. R. & Baran, P. S. C–H functionalization logic in total synthesis. *Chem. Soc. Rev.* **40**, 1976–1991 (2011).

3. Bakanas, I., Lusi, R. F., Wiesler, S., Cooke, J. H. & Sarpong, R. Strategic application of C–H oxidation in natural product total synthesis. *Nat. Rev. Chem.* **7**, 783–799 (2023).

4. Dorigo, A. E. & Houk, K. N. Transition structures for intramolecular hydrogen atom transfers: The energetic advantage of seven-membered over six-membered transition structures. *J. Am. Chem. Soc.* **109**, 2195–2197 (1987).

5. Dorigo, A. E. & Houk, K. N. On the relationship between proximity and reactivity. An ab initio study of the flexibility of the OH• + CH4 hydrogen abstraction transition state and a force-field model for the transition states of intramolecular hydrogen abstractions. *J. Org. Chem.* **53**, 1650–1664 (1988).

6. Tsui, E., Wang, H. & Knowles, R. R. Catalytic generation of alkoxy radicals from unfunctionalized alcohols. *Chem. Sci.* **11**, 11124–11141 (2020).

7. Xue, X. S., Ji, P., Zhou, B. & Cheng, J. P. The essential role of bond energetics in C–H activation/functionalization. *Chem. Rev.* **117**, 8622–8648 (2017).

8. Chang, L., An, Q., Duan, L., Feng, K. & Zuo, Z. Alkoxy radicals see the light: new paradigms of photochemical synthesis. *Chem. Rev.* **122**, 2429–2486 (2021).

9. Shi, Q.-Q., Tang, J.-J. & Gao, J.-M. Picrotoxane sesquiterpenoids: chemistry, chemo- and bio-syntheses and biological activities. *Nat. Prod. Rep.* **39**, 2096 (2022).

10. Gössinger, Edda. "Picrotoxanes." *Fortschritte der Chemie organischer Naturstoffe/Progress in the Chemistry of Organic Natural Products, Vol. 93* (2010).

11. Olsen, R. W. & Sieghart, W. International union of pharmacology. LXX. Subtypes of γ-aminobutyric acid A receptors: classification on the basis of subunit composition, pharmacology, and function. Update. *Pharmacol. Rev*. **60**, 243–260 (2008).

12. Ozoe, Y., Akamatsu, M., Higata, T., Ikeda, I., Mochida, K., Koike, K., Ohmoto, T., & Nikaido, T. Picrodendrin and related terpenoid antagonists reveal structural differences between ionotropic GABA receptors of mammals and insects. *Bioorg. Med. Chem.* **6**, 481-491 (1998).

13. Watanabe, I., Koike, K., Satou, T. & Nikaido, T. Nematocidal activity of picrodendrins against a species of Diplogastridae. *Biol. Pharm. Bull.* **22**, 1310 (1999).

14. Fernandez, F. et al. Pharmacotherapy for cognitive impairment in a mouse model of Down syndrome. *Nat. Neurosci.* **10**, 411 (2007).

15. Yoshiike, Y. et al. GABAA receptor-mediated acceleration of aging-associated memory decline in APP/PS1 mice and its pharmacological treatment by picrotoxin. *PloS One* **3**, e3029 (2008).

16. Pressly, B. et al. Comparison of the toxicokinetics of the convulsants picrotoxinin and tetramethylenedisulfotetramine (TETS) in mice. *Arch. Toxicol.* **94**, 1995–2007 (2020).

17. Wakamatsu, K., Kigoshi, H., Niiyama, K., Niwa, H. & Yamada, K. Stereocontrolled total synthesis of (+)-tutin and (+)-asteromurin A, toxic picrotoxane sesquiterpenes. *Tetrahedron* **42**, 5551–5558 (1986).

18. Wakamatsu, K., Kigoshi, H., Niiyama, K., Niwa, H. & Yamada, K. Stereocontrolled total synthesis of (+)-tutin, a toxic sesquiterpene of picrotoxane-type. *Tetrahedron Lett*. **25**, 3873–3874 (1984).

19. Krische, M. J. & Trost, B. M. Transformations of the picrotoxanes: the synthesis of corianin and structural analogues from picrotoxinin. *Tetrahedron* **54**, 7109–7120 (1998).

20. Trost, B. M. & Krische, M. J. General strategy for the asymmetric synthesis of the picrotoxanes. *J. Am. Chem. Soc.* **118**, 233–234 (1996).

21. Niwa, H., Wakamatsu, K., Hida, T., Niiyama, K., Kigoshi, H., Yamada, M., Nagase, H., Suzuki, M. & Yamada, K. Stereocontrolled total synthesis of (−)-Picrotoxinin and (+)-Coriamyrtin via a common isotwistane intermediate. *J. Am. Chem. Soc.* **106**, 4547–4552 (1984).

22. Tanaka, K., Uchiyama, F., Sakamoto, K. & Inubushi, Y. Total synthesis of Corianin. *J. Am. Chem. Soc.* **104**, 4965–4967 (1982).

23. Ikeuchi, K., Haraguchi, S., Fuji, R., Yamada, H., Suzuki, T. & Tanino, K. Total synthesis of (+)-Coriamyrtin via a desymmetrizing strategy involving a 1,3-cyclopentanedione moiety. *Org. Lett.* **25**, 2751–2755 (2023).

24. Tong, G., Griffin, S., Sader, A., Crowell, A. B., Beavers, K., Watson, J., Buchan, Z., Chen, S. & Shenvi, R. A. C5 methylation confers accessibility, stability and selectivity to picrotoxinin. *Nature Commun*. **14**, 8308 (2023).

25. Tong, G. & Shenvi, R. A. Revision of the unstable picrotoxinin hydrolysis product. *Angew. Chem. Int. Ed.* **60**, 19113 (2021).

26. Conroy, H. Total synthesis of picrotoxinin. *J. Am. Chem. Soc.* **79**, 5550 (1957).

27. Fields, B. A., Reeve, J., Bartholomaeus, A. & Mueller, U. Human pharmacokinetic study of tutin in honey; a plant-derived neurotoxin. *Food Chem. Toxicol.* **72**, 234–241 (2014).

28. Crossley, S. W. M., Tong, G., Lambrecht, M., Burdge, H. E. & Shenvi, R. A. Synthesis of picrotoxinin via late-stage strong bond activations. *J. Am. Chem. Soc.* **142**, 11376–11381 (2020).

29. Boto, A., Hernández, D., Hernández, R. & Suárez, E. β-Fragmentation of primary alkoxyl radicals versus hydrogen abstraction: synthesis of polyols and α, ω-differently substituted cyclic ethers from carbohydrates. *J. Org. Chem.* **68**, 5310–5319 (2003).

30. Corey, E. J.; Cheng, X.-M. The Logic of Chemical Synthesis, John Wiley & Sons, New York, 1995

31. Salatin, T. D. & Jorgensen, W. L. Computer-assisted mechanistic evaluation of organic reactions. 1. Overview. *J. Org. Chem.* **45**, 2043–2051 (1980).

32. Wei, J. N., Duvenaud, D., & Aspuru-Guzik, A. Neural networks for the prediction of organic chemistry reactions. *ACS Cent. Sci.* **2**, 725−732 (2016).

33. Szymkuć, S., Gajewska, E. P., Klucznik, T., Molga, K., Dittwald, P., Startek, M., Bajczyk, M., & Grzybowski, B. A. Computer-assisted synthetic planning: The end of the beginning. *Angew. Chem. Int. Ed.* **55**, 5904−5937 (2016).

34. Zhang, P., Eun, J., Elkin, M., Zhao, Y., Cantrell, R. L., & Newhouse, T. R. A neural network model informs the total synthesis of clovane sesquiterpenoids. *Nature Synthesis* **2**, 527–534 (2023).

35. Coley, C. W., Green, W. H. & Jensen, K. F. Machine learning in computer-aided synthesis planning. *Acc. Chem. Res*. **51**, 1281–1289 (2018).

36. Coley, C. W., Rogers, L., Green, W. H. & Jensen, K. F. Computer-assisted retrosynthesis based on molecular similarity. *ACS Cent. Sci.* **3**, 1237–1245 (2017).

37. Cadeddu, A., Wylie, E. K., Jurczak, J., Wampler-Doty, M. & Grzybowski, B. A. Organic chemistry as a language and the implications of chemical linguistics for structural and retrosynthetic analyses. *Angew. Chem. Int. Ed.* **53**, 8108-8112 (2014).

38. Huang, J., Bunel, E. & Faul, M. M. Palladium-catalyzed r-vinylation of carbonyl compounds. *Org. Lett.* **9**, 4343–4346 (2007).

39. Murphy, S. K., Park, J.-W., Cruz, F. A. & Dong, V. M. Rh-catalyzed C–C bond cleavage by transfer hydroformylation. *Science* **347**, 56–60 (2015).

40. Krische, M. J. & Trost, B. M. Total synthesis of methyl picrotoxate via the palladium catalyzed enyne cycloisomerization reaction. *Tetrahedron* **54**, 3693 (1998).

41. Trost, B. & Krische, M. J. Palladium-catalyzed enyne cyclo-isomerization reaction in an asymmetric approach to the picrotoxane sesquiterpenes. 2. Second-generation total syntheses of corianin, picrotoxinin, picrotin, and methyl picrotoxate. *J. Am. Chem. Soc.* **121**, 6131 (1999).

42. Eckart, C. The theory of collisions. *Phys. Rev.* **35**, 1303 (1930).

43. Garrett, B. C. & Truhlar, D. G. Semiclassical tunneling calculations. *J. Phys. Chem*. **83**, 2921–2926 (1979).

44. Eyring, H. The activated complex in chemical reactions. *J. Chem. Phys.* **3**, 107–115 (1935).

45. Truhlar, D. G., Hase, W. L. & Hynes, J. T. Current status of transition-state theory. J. *Phys. Chem.* **87**, 2664–2682 (1983).

46. Brun, P. & Waegell, B. Heterocyclisation intramoleculaire d'alcools possedant un squelette cedranique. Oxydation par le tetraacetate de plomb et par l'oxyde de mercure et le brome. *Tetrahedron* **32**, 1137–1145 (1976).

47. Zhao, Y. & Truhlar, D. G. The M06 suite of density functionals for main group thermochemistry, thermochemical kinetics, noncovalent interactions, excited states, and transition elements: two new functionals and systematic testing of four M06-class functionals and 12 other functionals. *Theor. Chem. Acc.* **120**, 215–241 (2008).

48. Marenich, A. V., Cramer, C. J. & Truhlar, D. G. Universal solvation model based on solute electron density and on a continuum model of the solvent defined by the bulk dielectric constant and atomic surface tensions. *J. Phys. Chem. B* **113**, 6378–6396 (2009).

49. Truce, W. E., Campbell, R. W. & Norell, J. R. Sulfene, an intermediate in the alcoholysis of methanesulfonyl chloride. *J. Am. Chem. Soc.* **86**, 288 (1964).

50. Wakamatsu, K.; Kigoshi, H.; Niiyama, K.; Niwa, H.; & Yamada, K. "Stereocontrolled total synthesis of (+)-tutin and (+)-asteromurin A, toxic picrotoxane sesquiterpenes" *Tetrahedron* **1986**, *42*, 5551–5558.

51. Meng, S.-S. et al. Chiral phosphoric acid catalyzed highly enantioselective desymmetrization of 2-substituted and 2,2-disubstituted 1,3-diols via oxidative cleavage of benzylidene acetals. *J. Am. Chem. Soc.* **136**, 12249–12252 (2014).

52. Forbes, C. P., Goosen, A. & Laue, H. A. H. Hypoiodite reaction: Kinetic study of the reaction of 1,1-diphenylethylene with mercury(II) oxide-iodine. *J. Chem. Soc. Perkin I* 2350–2353 (1974).

53. Lee, S. & Fuchs, P. L. An efficient C−H oxidation protocol for α-hydroxylation of cyclic steroidal ethers. *Org. Lett.* **6**, 1437–1440 (2004).

54. Wang, J. B. & Suginome, H. Intramolecular β, γ-addition of allylic alkoxyl radicals. A new general synthesis of α-lodoepoxides by photolysis of allylic alcohol hypoiodites in the presence of mercury(II) oxide, iodine and pyridine in benzene. *J. Chem. Soc., Chem. Commun.* 1629–1631 (1990).

55. Frisch, M. J., Pople, J. A. & Binkley J. S. Self-consistent molecular orbital methods 25. Supplementary functions for Gaussian basis sets. *J. Chem. Phys.* **80**, 3265–3269 (1984).

56. Liu, F. et al. Hydrogen abstraction by alkoxyl radicals: computational studies of thermodynamic and polarity effects on reactivities and selectivities. *J. Am. Chem. Soc.* **144**, 6802–6812 (2022).

57. Strieth-Kalthoff, F., Szymkuć, S., Molga, K., Aspuru-Guzik, A., Glorius, F., & Grzybowski, B. A. Artificial intelligence for retrosynthetic planning needs both data and expert knowledge. *J. Am. Chem. Soc.* **146**, 11005-11017 (2024).

58. Boger, D. L., Miyazaki, S., Kim, S. H., Wu, J. H., Castle, S. L., Loiseleur, O., & Jin, Q. Total synthesis of the vancomycin aglycon. *J. Am. Chem. Soc.* **121**, 43, 10004–10011 (1999).

59. Zhong, W., Yang, Z., & Chen, C. Y.-C. Retrosynthesis prediction using an end-to-end graph generative architecture for molecular graph editing. *Nature Commun*. **14**, 3009 (2023).

60. Ihlenfeldt, W.-D., & Gasteiger, J. Computer-assisted planning of organic syntheses: The second generation of programs. *Angew. Chem. Int. Ed. Engl.* **34***,* 2613-2633 (1995).

61. Wang, Z., Zhang, W., & Liu, B. Computational analysis of synthetic planning: Past and future. *Chin. J. Chem*. **39**, 11, 3127-3143 (2021).